Supplementary Data for

Tuning graphene doping by carbon monoxide intercalation at the Ni(111) interface

Simone Del Puppo[a], Virginia Carnevali[a,b,1], Daniele Perilli[c], Francesca Zarabara[a], Alberto Lodi Rizzini[b], Gabriele Fornasier[a,b], Erik Zupanič[d], Sara Fiori[a,b], Laerte L. Patera[a,b,2], Mirco Panighel[b], Sunil Bhardwaj[b], Zhiyu Zou[b], Giovanni Comelli[a,b], Cristina Africh[b], Cinzia Cepek[b], Cristiana Di Valentin[c], Maria Peressi[a,*]

[a] *Department of Physics, University of Trieste, via A. Valerio 2, I-34127, Trieste, Italy*

[b] *CNR-IOM, Laboratorio TASC, S.S. 14 Km 163.5, Basovizza, I-34149, Trieste, Italy*

[c] *Department of Materials Science, University of Milano-Bicocca, via R. Cozzi 55, I-20125 Milano, Italy*

[d] *Jožef Stefan Institute, Jamova 39, SI-1000 Ljubljana, Slovenia*

[1] *Present address: Central Michigan University, Mount Pleasant, Michigan 48858, United States.*

[2] *Present address: Department of Chemistry, Technical University of Munich, Lichtenbergstraße 4, 85748 Garching, Germany.*

* *Corresponding author. E-mail address: peressi@units.it*

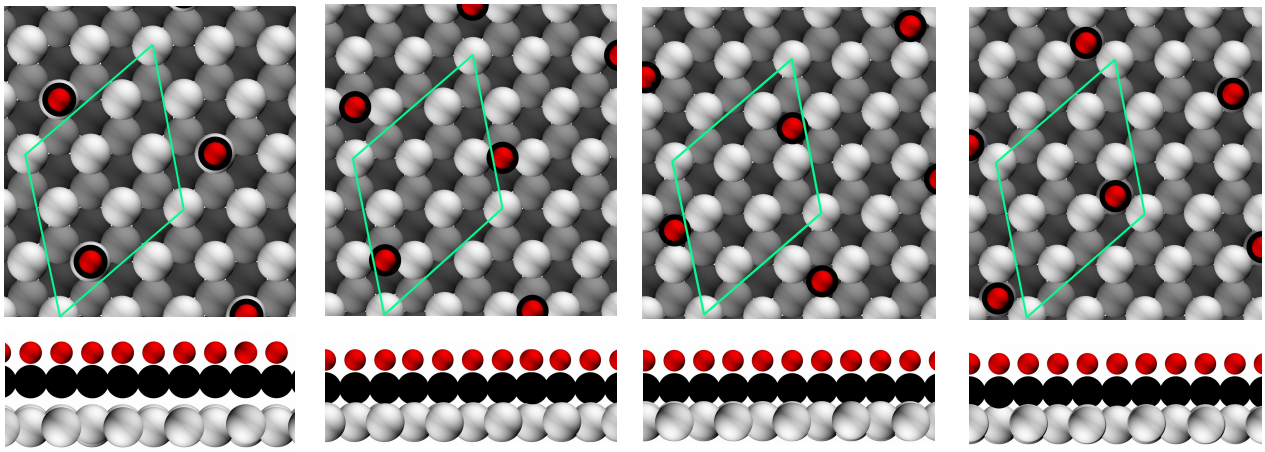

Figure S1: Stable high-symmetry adsorption patterns of CO on Ni(111) surface in absence of Gr capping for a CO coverage of 0.14 ML, obtained from DFT calculations in a rhombic $(\sqrt{7} \times \sqrt{7})R19^o$ simulation cell. From left to right: top, bridge, fcc, hcp.

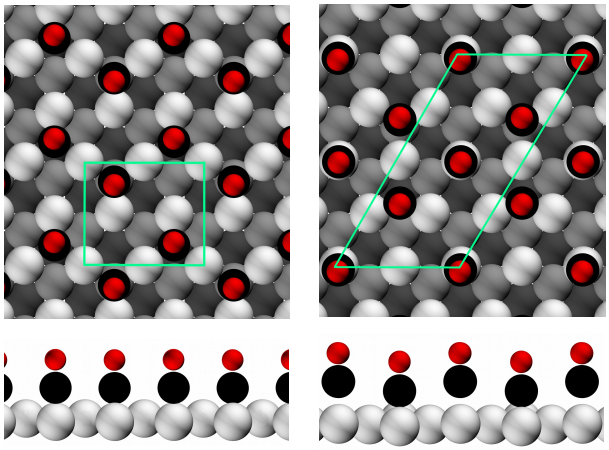

Figure S2: Two different stable adsorption patterns of CO on Ni(111) surface in absence of Gr capping for a CO coverage of 0.50 ML, obtained from DFT calculations in a rectangular $(2 \times \sqrt{3})$ (configuration A: 50%-50% fcc-hcp sites) and parallelogrammatic $c(4 \times 2)$ (configuration B: 50%-50% top-hollow) simulation cells.

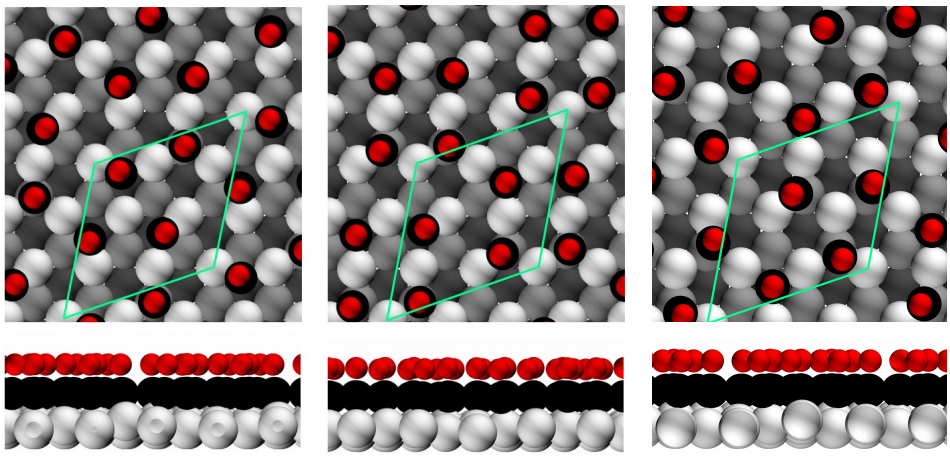

Figure S3: Three different stable adsorption patterns of CO on Ni(111) surface in absence of Gr capping for a CO coverage of 0.57 ML, obtained from DFT calculations in the rhombic $(\sqrt{7} \times \sqrt{7})R19^o$ simulation cell. From left to right: 1hcp+3fcc, 2hcp+2fcc, 3hcp+1fcc.

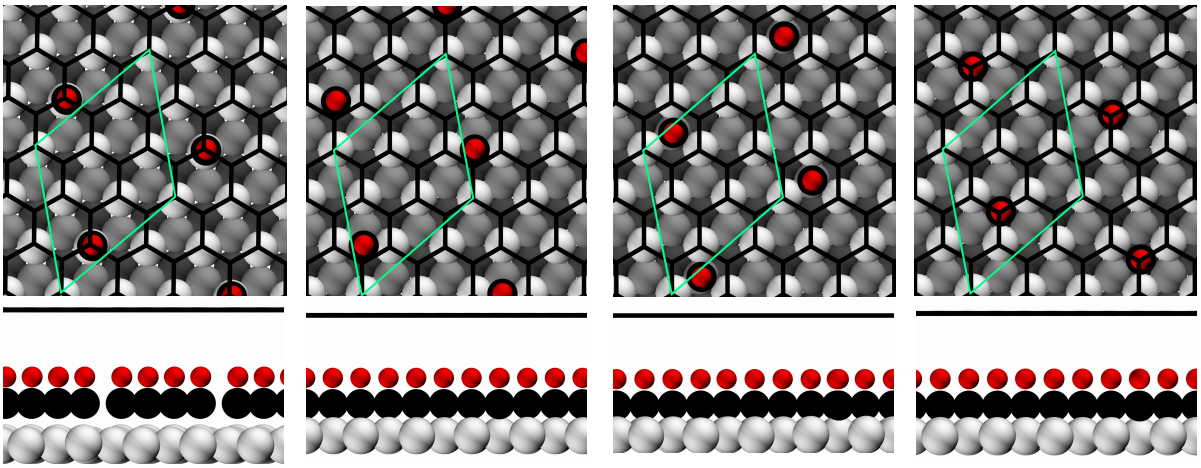

Figure S4: Adsorption configuration of CO on Ni(111) surface in presence of Gr capping for a CO coverage of 0.14 ML, obtained from DFT calculations in the rhombic $\left(\sqrt{7}\times\sqrt{7}\right)R19^{o}$ simulation cell. From left to right: top, bridge, hcp, fcc. Fcc and hcp are stable adsorption sites, whereas top and bridge configurations are obtained forcing the in-plane positions of the CO molecules.

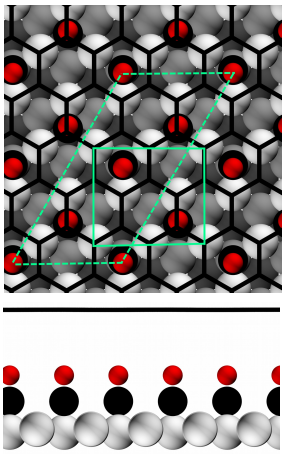

Figure S5: Stable adsorption pattern of CO on Ni(111) surface in presence of Gr capping for a CO coverage of 0.50 ML, obtained from DFT calculations in a rectangular $\left(2\times\sqrt{3}\right)$ cell. The (4× 2) cell, with a size which is twice the rectangular one, is indicated with a dashed line.

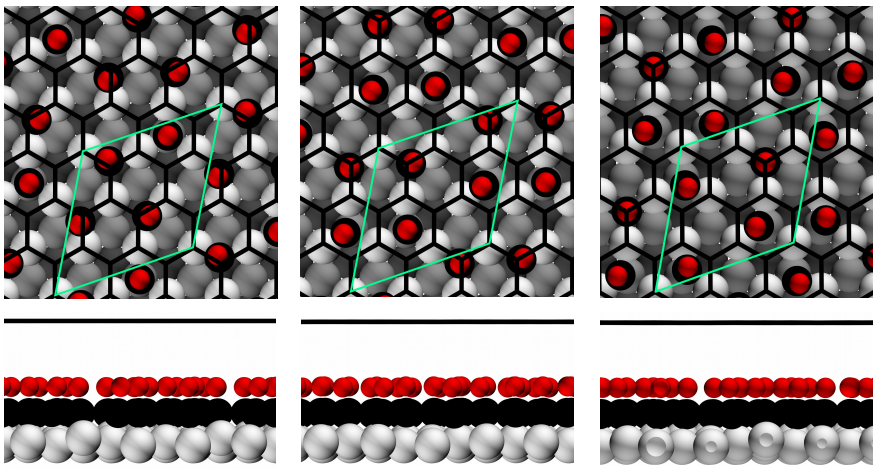

Figure S6: Stable adsorption pattern of CO on Ni(111) surface in presence of Gr capping for a CO coverage of 0.57 ML, obtained from DFT calculations in the rhombic $\left(\sqrt{7}\times\sqrt{7}\right)R19^{o}$ simulation cell. From left to right: 1hcp+3fcc, 2hcp+2fcc, 3hcp+1fcc.

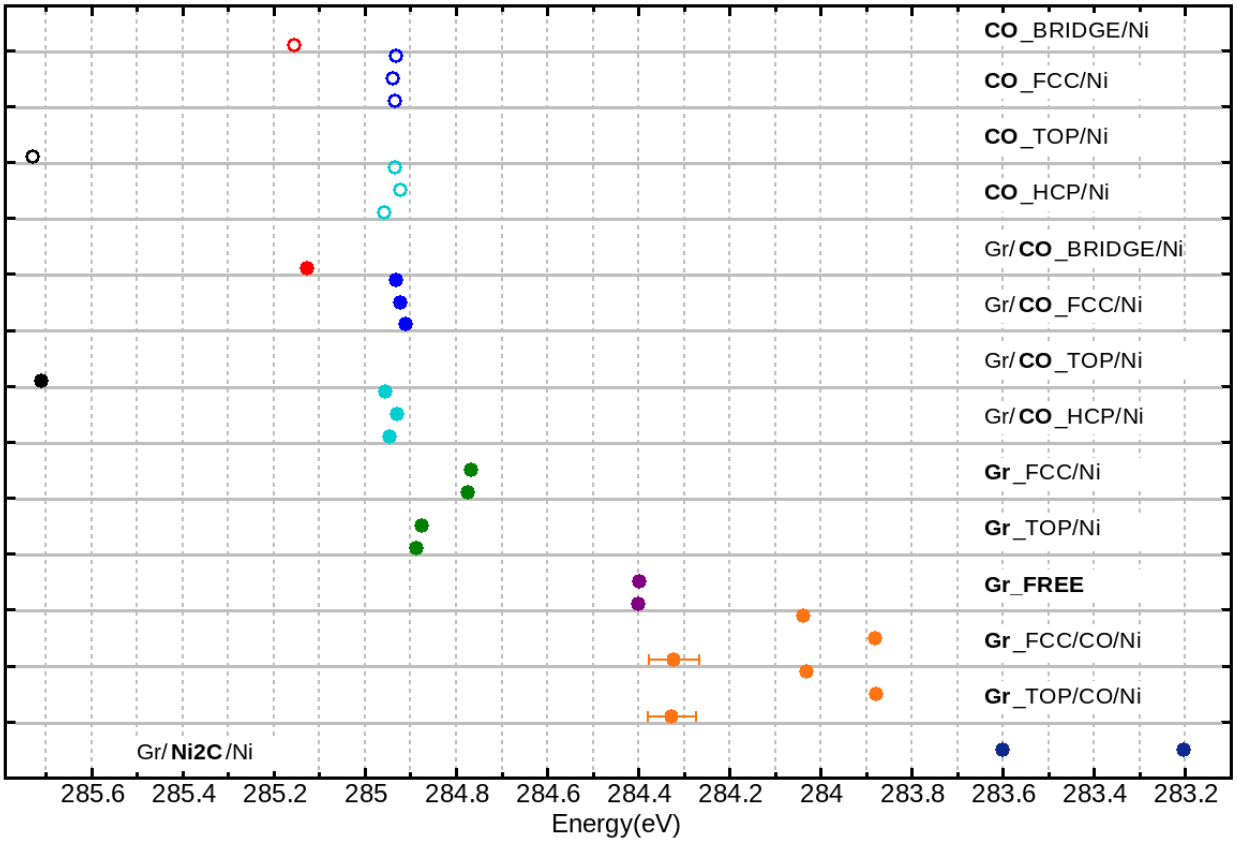

Figure S7: Details of DFT calculated C 1s core level binding energies (horizontal axis) for C atoms in CO/Ni, Gr/Ni, Gr/CO/Ni, Gr/Ni_2C/Ni.
The results are separated in different panels: each panel refers to a specific system and a specific C type, indicated in the label (bold fonts are used to unambiguously distinguish which C type we refer to). The same color code of Fig. 2 (XPS spectrum) of the Main Text is used: purple for C atoms of free standing Gr; orange for C atoms of Gr decoupled by Ni after CO intercalation; green for C atoms of Gr directly interacting with Ni; light blue for C atoms of CO at (or close to) fcc or hcp sites; red for C atoms of CO at bridge sites; black for C atoms of CO at top sites, dark blue for C atoms of a carbide layer between Gr and Ni. Filled/open symbols for C atoms of CO indicate configurations with/without Gr capping, respectively. For the C atoms of Gr we show separately the results for the two sublattices, having top and fcc registry with respect to the Ni(111) surface.
In each panel we distinguish results obtained in different simulation cells, distributing them on the vertical axis for visualization purposes. In particular, from bottom to top within each panel: i) for systems including CO we report the results for coverage of 0.14 ML, 0.50 ML, 0.57 ML, respectively; ii) for free Gr and Gr/Ni we report the results obtained in the $(\sqrt{7} \times \sqrt{7})R19^o$ cell and in a cell multiple of the $(2 \times \sqrt{3})$, respectively (this choice guarantees that a core-excited C atom is well separated from its images in the adjacent periodically repeated cells); iii) the results for Gr/Ni_2C/Ni have been obtained in the cell described in [1].
The error bar on the C 1s peak position of Gr in Gr/CO(θ=0.14ML)/Ni (orange) indicates the variation with the particular choice of the C atom of Gr. In all the other cases the variations are negligible.

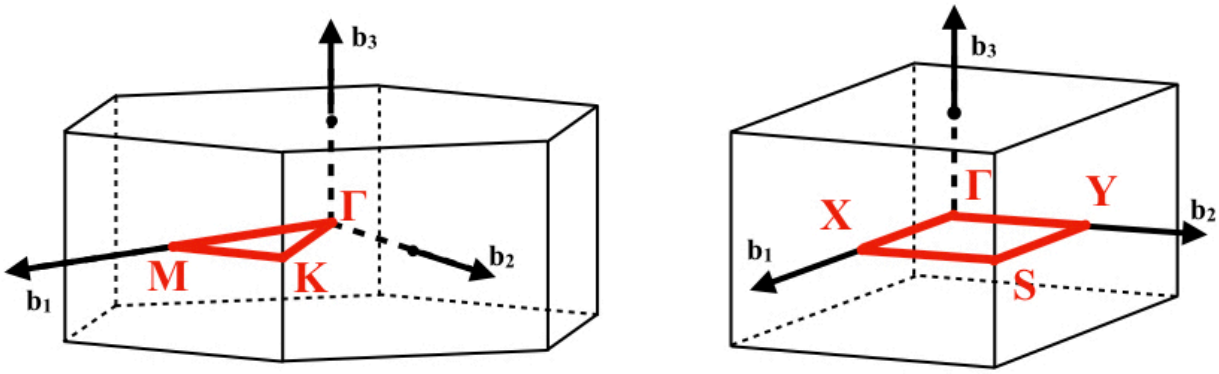

Figure S8: Brillouin zones of the hexagonal and orthorhombic cells with the indication of the paths followed for the band structure representations in Figure 3 of the Main Text.

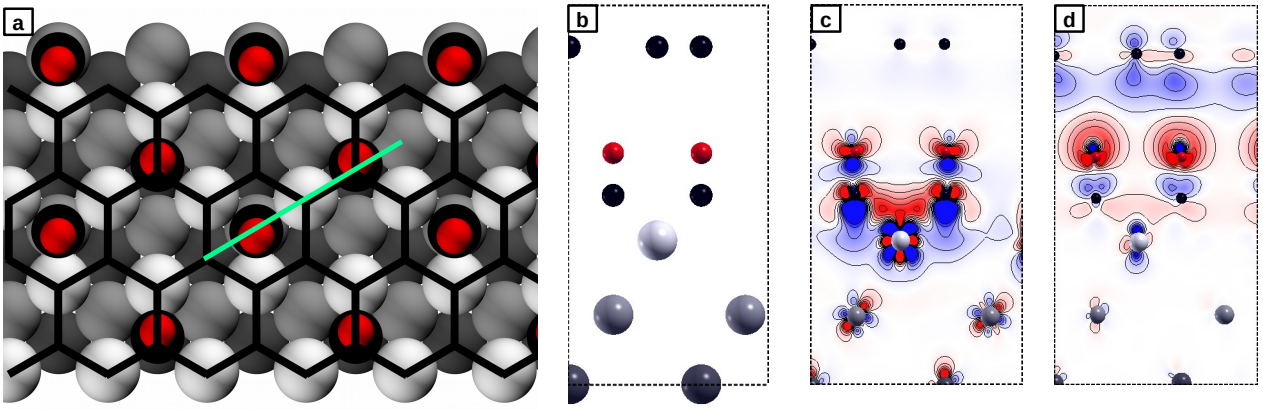

Figure S9: Stick-and-ball model (a,b) and electron density difference plots (c,d) for a stable adsorption configuration for a CO coverage of 0.50 ML. Stick-and-ball model: (a) top view, with the indication of the plane considered for the side view; (b) side view. Plots in the plane (b) for two different electron density differences, obtained by subtracting to the electron density distribution of the whole system: (c) the sum of the three constituents (Gr, CO, Ni); (d) the sum of CO/Ni and Gr. The atomic positions are always kept frozen in the position optimized in the entire system. Red/blue indicates abundance/depletion of electrons. The electron density difference isosurfaces are plotted at +/−0.015 $|e|/a_0^3$ and at +/−0.002 $|e|/a_0^3$ in (c) and (d), respectively. The smallest scale in (d) allows to appreciate the very small electron transfer from Gr to the intercalated CO.

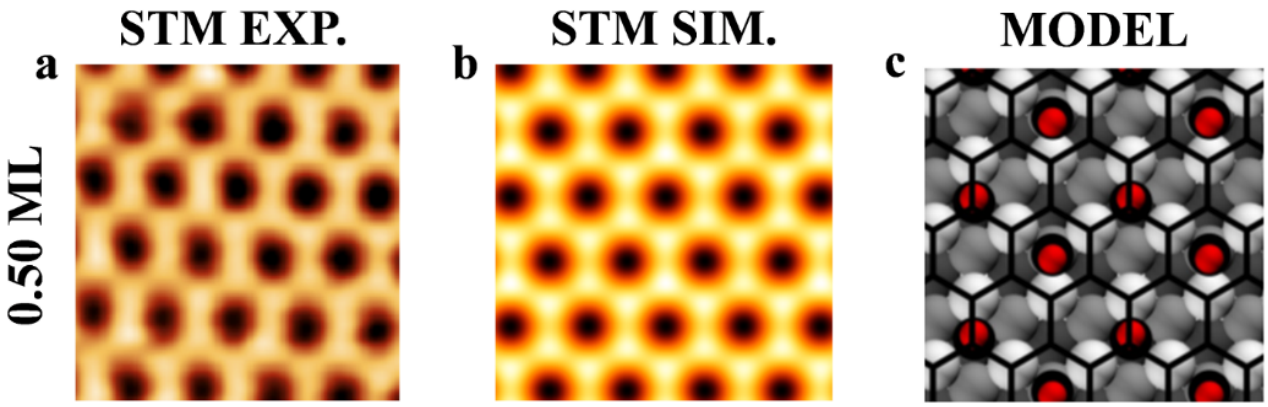

Figure S10: (a) Experimental and (b) simulated STM images of the Gr/CO/Ni(111) at 0.50 ML. (c) Stick and ball model in top view. Experimental parameters: (a) I = 1 nA, V_{bias} = +0.4 V; Computational parameters: V_{bias} = +0.4 V; ILDOS plot on a plane lying at 2 Å above graphene.

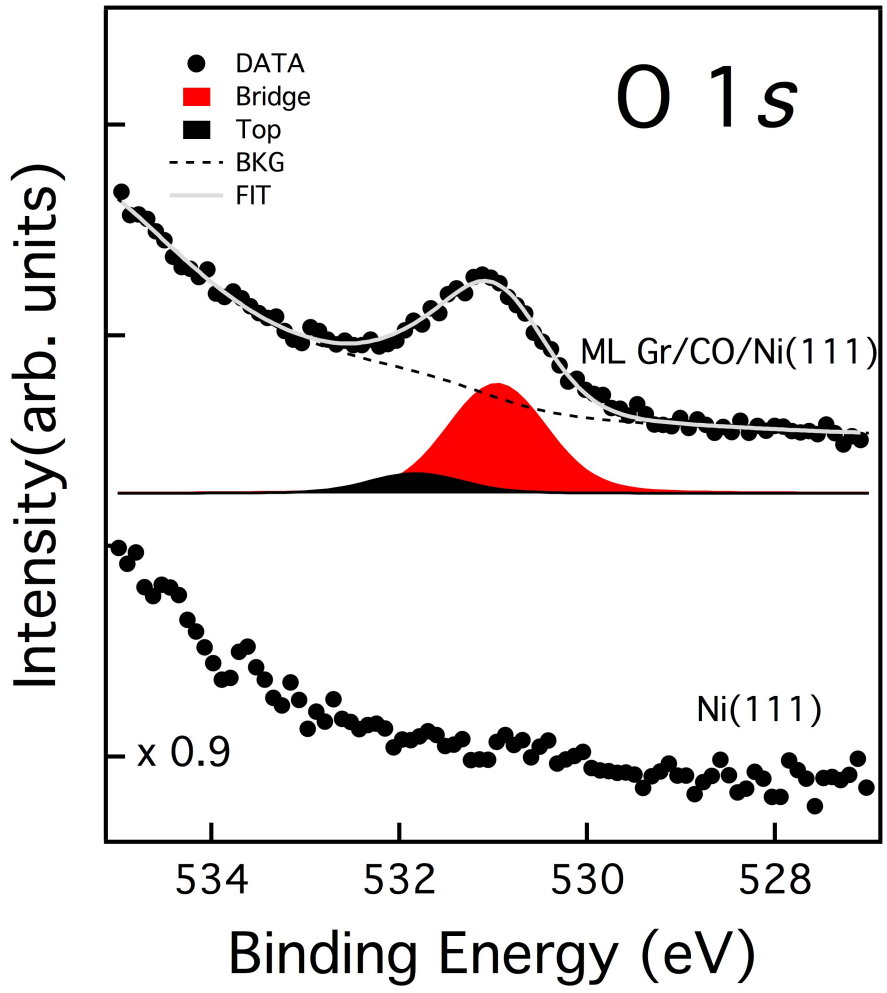

Figure S11: O 1s XPS spectra

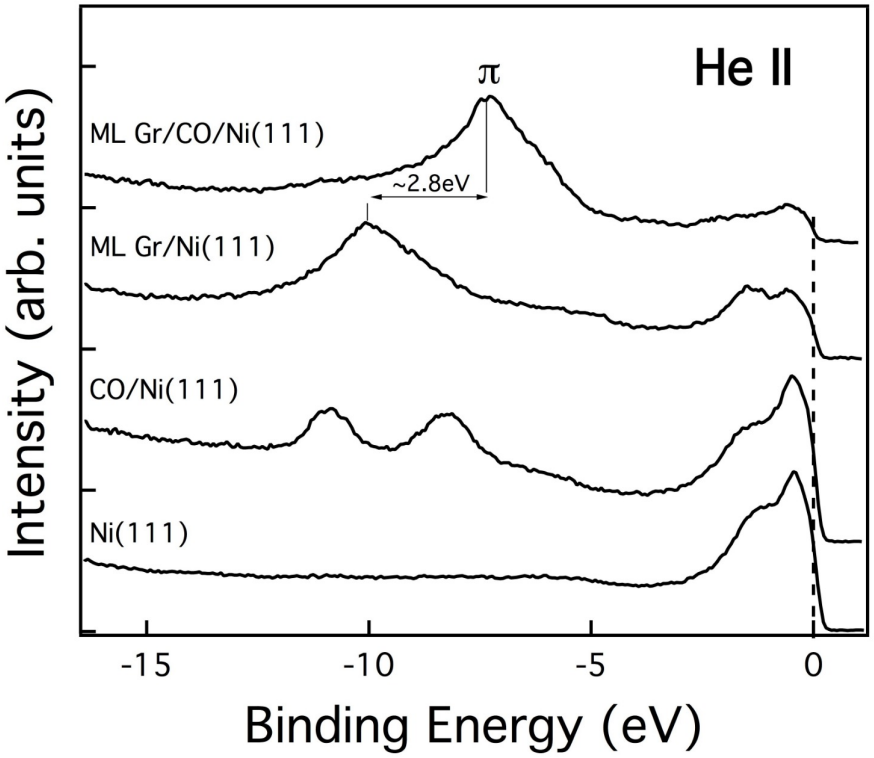

Figure S12: Normal emission valence band photoemission spectra of Ni(111), CO/Ni(111), Gr/Ni(111) and Gr/CO/Ni(111).

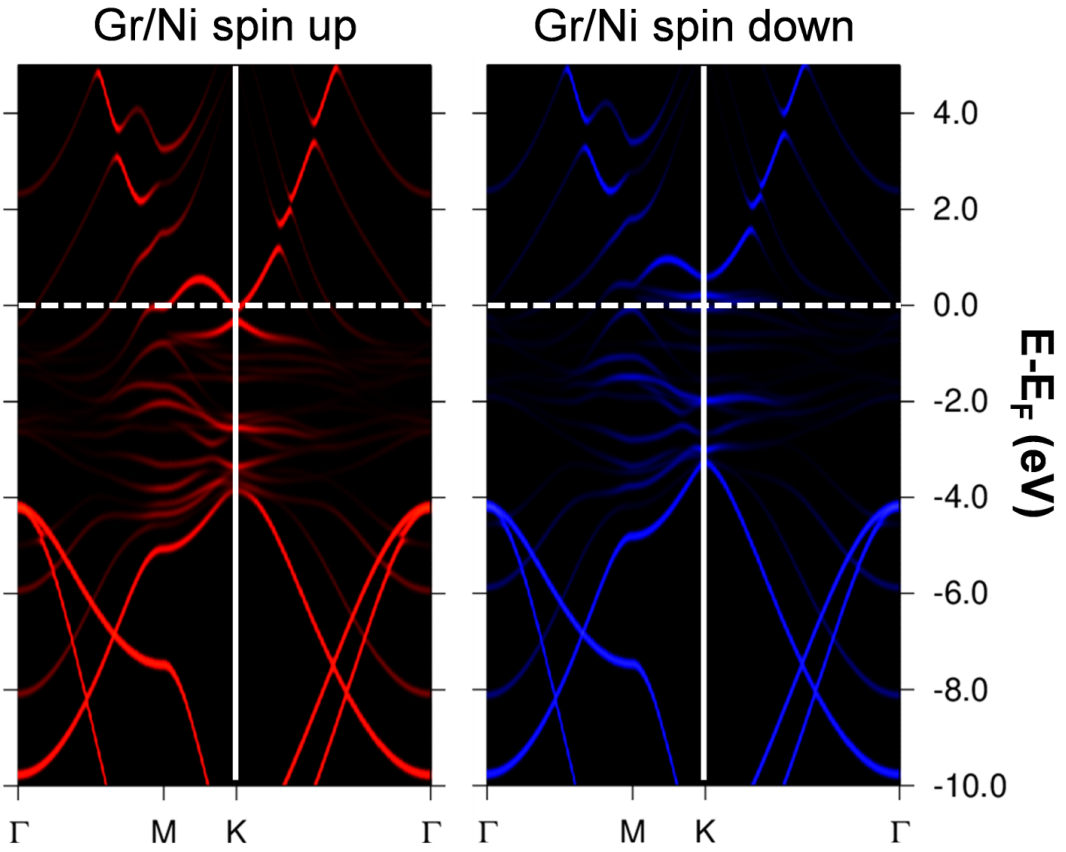

Figure S13: Spin-resolved Gr-projected band structure along the high symmetry path for Gr/Ni.

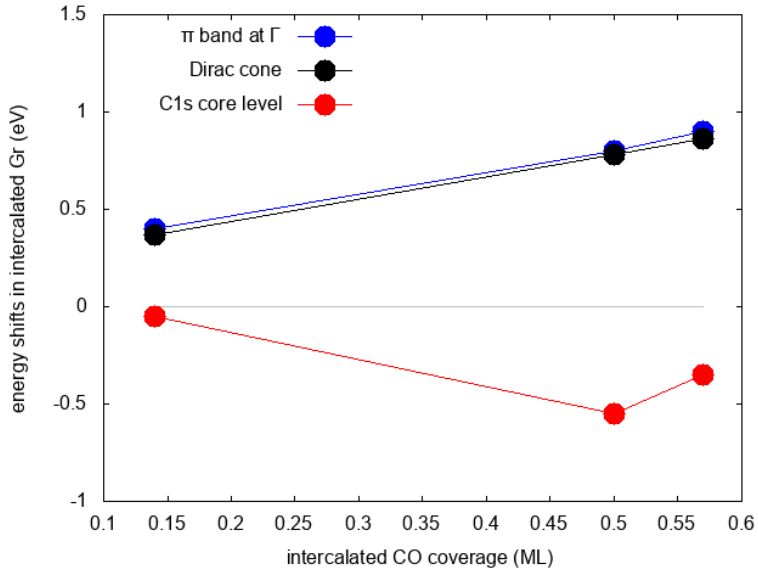

Figure S14: Energy shifts of the Gr π band bottom at Γ, of the energy position of the Dirac cone with respect to the Fermi energy, of the Gr C 1s binding energy. The zero level corresponds to free Gr. The data of the Dirac cone shifts are the same reported in Figure 4b.

Table S1: Intercalation energy in eV (see main text for definition) for CO molecules at Gr/Ni(111) interface, and adsorption energy for the molecules adsorbed on Ni(111) in absence of Gr capping. In the latter case, the results with and without van der Waals corrections are shown.
For each coverage, the results for different configurations are reported. The intercalation energy for 0.14 ML for top and bridge sites, marked with an asterisk, has been calculated by constraining the in-plane position of CO, since the two sites are not stable adsorption sites in presence of Gr capping. The configuration at 0.50 ML with 1hcp+1fcc+2top which is stable in absence of Gr capping, it is not in presence of Gr capping.

Θ (ML)		$E_{interc\ CO}$ (eV) (with vdW)	$E_{ads\ CO}$ (eV) (no Gr, with vdW)	$E_{ads\ CO}$ (eV) (no Gr, no vdW)
0.14 ML	top	0.15*	-1.86	-1.56
	bridge	-0.15*	-2.08	-1.80
	fcc	-0.30	-2.22	-1.91
	hcp	-0.34	-2.24	-1.93
0.50 ML	A: 1hcp+1fcc	-1.78	-2.26	-1.90
	B: 1hcp+1fcc+2top	-	-1.98	-1.62
0.57 ML	1hcp+3fcc	-1.76	-2.16	-1.78
	2hcp+2fcc	-1.75	-2.15	-1.77
	3hcp+1fcc	-1.78	-2.15	-1.77

Table S2: Experimental and DFT calculated C1s XPS peaks. In the experimental column, in square brackets, values from Ref. [2] are reported, in addition to the values obtained in the present work. The calculated values have been aligned with the experimental peaks for the non-interacting (free-standing) Gr. In the DFT column, for each coverage we report the value mediated over different inequivalent C atoms. We highlight in bold the values reported for comparison with experiments in the spectrum of Figure 2. See also Figure S7 for further details.
(i) free fitting parameter in the deconvolution of the experimental spectrum;
(ii) fixed parameter;
(iii) free fitting parameter;
(iv) CO bridge and hollow fitted as a single peak.

C1s	Exp (eV) [2]	DFT (eV)	
		Gr/CO/Ni(111)	CO/Ni(111)
Gr decoupled by CO	283.8(i) [283.9]	284.35 [0.14ML] **283.85 [0.50ML]** 284.05 [0.57ML]	-
Gr non interacting	284.4(ii) [284.3]	**284.40**	-
Gr/Ni	284.8(iii) [285.0]	**284.80 [fcc]** **284.90 [top]**	-
CO bridge	285.3(iv) [285.4]	**285.15 [0.14ML]**	285.15
CO hollow		284.95 [0.14ML] **284.95 [0.50ML]** 284.95 [0.57ML]	284.95 [0.14ML] 284.95 [0.50ML] 284.95 [0.57ML]
CO top	285.9 [286.0]	**285.70 [0.14ML]**	285.70
carbide	283.2 [283.0-.5]	283.20 283.60	-

Table S3: CO stretching frequencies (in cm^{-1}) and bond distance (in Å) for CO/Ni and Gr/CO/Ni at 0.14 ML CO coverage. Each line is referred to a different stable CO adsorption position with respect to the metal substrate: fcc and hcp.

0.14 ML	CO/Ni		Gr/CO/Ni		$\Delta\nu_{C\text{-}O}$ (cm^{-1})
	dist. C-O (Å)	**$\nu_{C\text{-}O}$ (cm^{-1})**	**dist. C-O (Å)**	**$\nu_{C\text{-}O}$ (cm^{-1})**	
CO fcc	1.20	1744.3	1.21	1729.8	-14.5
CO hcp	1.20	1712.1	1.21	1686.1	-26.0

Table S4: CO stretching frequencies (in cm^{-1}) and bond distance (in Å) for CO/Ni and Gr/CO/Ni at 0.50 ML CO coverage. Each line is referred to a different CO adsorption position with respect to the metal substrate: fcc and hcp.

0.50 ML	CO/Ni		Gr/CO/Ni		$\Delta\nu_{C\text{-}O}$ (cm^{-1})
	dist. C-O (Å)	**$\nu_{C\text{-}O}$ (cm^{-1})**	**dist. C-O (Å)**	**$\nu_{C\text{-}O}$ (cm^{-1})**	
CO fcc	1.19	1801.3	1.20	1753.5	-47.8
CO hcp	1.20	1790.5	1.20	1751.0	-39.5

Table S5: CO stretching frequencies (in cm^{-1}) and bond distance (in Å) for CO/Ni and Gr/CO/Ni at 0.57 ML CO coverage in the configuration 3hcp+1fcc. Each line is referred to a different CO adsorption position with respect to the metal substrate: fcc and hcp.

0.57 ML	CO/Ni		Gr/CO/Ni		$\Delta\nu_{C\text{-}O}$ (cm^{-1})
	dist. C-O (Å)	**$\nu_{C\text{-}O}$ (cm^{-1})**	**dist. C-O (Å)**	**$\nu_{C\text{-}O}$ (cm^{-1})**	
CO fcc	1.19	1791.7	1.20	1752.5	-39.2
CO hcp	1.19	1792.2	1.20	1758.8	-33.4
CO hcp	1.19	1793.0	1.20	1754.8	-38.2
CO hcp	1.19	1793.4	1.20	1753.9	-39.5

Reference:

[1] S. Stavrić, S. Del Puppo, Ž. Šljivančanin, M. Peressi, First-principles study of nickel reactivity under two-dimensional cover: Ni_2C formation at rotated graphene/Ni(111) interface, Phys. Rev. Materials **5** (2021) 014003.

[2] Mingming Wei et al., Modulation of Surface Chemistry of CO on Ni(111) by Surface Graphene and Carbidic Carbon, J. Phys. Chem. C **119** (2015) 13590−13597.